

## Article

# Pool Fire Suppression Using CO<sub>2</sub> Hydrate

Olga Gaidukova <sup>1</sup>, Sergey Misyura <sup>1,2,\*</sup>, Igor Donskoy <sup>3</sup> , Vladimir Morozov <sup>2</sup> and Roman Volkov <sup>1</sup> <sup>1</sup> Heat Mass Transfer Laboratory, National Research Tomsk Polytechnic University, 634050 Tomsk, Russia<sup>2</sup> Kutateladze Institute of Thermophysics, 630090 Novosibirsk, Russia<sup>3</sup> Melentiev Energy Systems Institute SB RAS, 130 Lermontov Street, 664033 Irkutsk, Russia

\* Correspondence: misura@itp.nsc.ru

**Abstract:** This paper presents experimental findings on heat and mass transfer, phase transitions, and chemical reactions during the interaction of CO<sub>2</sub> hydrate in powder granules and tablets with burning liquid fuels and oil. The experiments involved CO<sub>2</sub> hydrate tablets and spheres made of pressed granules. The fire containment and suppression times were established experimentally. Using the gas analysis data, we studied the effects of the mitigation of anthropogenic emissions from the combustion of liquids and their suppression by gas hydrates. We also compared the performance of water aerosol, foaming agent emulsion, snow, ice, and CO<sub>2</sub> hydrate samples as laboratory-scale fire suppressants. The paper further describes the numerical modeling of the CO<sub>2</sub> hydrate dissociation during liquid fuel combustion. The rapid carbon dioxide release is shown to prevent the oxidizer from the combustion zone. The suppression of a flame using powder with a granule size of 3 mm requires 20-times less carbon dioxide hydrate than in the case of pressed tablets. Effective conditions are identified for using CO<sub>2</sub> hydrates to extinguish fires involving flammable liquids and most common fuels.

**Keywords:** CO<sub>2</sub> hydrate granules; fire suppression; oil; liquid fuel; emission mitigation; closed-loop fire suppression systems



**Citation:** Gaidukova, O.; Misyura, S.; Donskoy, I.; Morozov, V.; Volkov, R. Pool Fire Suppression Using CO<sub>2</sub> Hydrate. *Energies* **2022**, *15*, 9585. <https://doi.org/10.3390/en15249585>

Academic Editor: Michael Liberman

Received: 16 November 2022

Accepted: 14 December 2022

Published: 16 December 2022

**Publisher's Note:** MDPI stays neutral with regard to jurisdictional claims in published maps and institutional affiliations.



**Copyright:** © 2022 by the authors. Licensee MDPI, Basel, Switzerland. This article is an open access article distributed under the terms and conditions of the Creative Commons Attribution (CC BY) license (<https://creativecommons.org/licenses/by/4.0/>).

## 1. Introduction

Like any other major disaster, fire threatens social development and public safety [1–3], so industrial fire protection has become an integral part of the production process. Fires involving flammable liquids are the most frequent technological emergencies [4,5], as liquid fuels may leak during their production, storage, and transportation [6]. Liquid fuels are difficult to extinguish due to their high heat release, evaporation, and burnout rates, as well as fluidity [7]. What makes it even worse is that the combustion products of such liquids contain harmful substances, which are hazardous for human life and health. During a fire, chemical substances that are stored on site or synthesized as part of uncontrolled chemical reactions can form toxic environments enlarging at a high rate. Liquid fuels (gasoline, kerosene, and diesel fuel) are extensively used in the transportation, metallurgy, electric power, aerospace, and chemical industries [8–10]. However, the wide use of oil fuels has drastically increased their fire hazard, so the industrial fire safety design is becoming increasingly critical [8].

Fire extinguishing agents are an important part of active fire safety [11–13], with foam-based agents being the most popular when it comes to fires involving liquid fuels [14–16]. With a large-scale fire source, however, it is difficult to cover the whole of it with a foam extinguishing agent, which makes fire suppression less effective [17]. Water mist, which is also used in fire extinguishing, fills the fire zone from top to bottom, and this is a significant advantage for the suppression of three-dimensional fires. However, water mist is less effective than foam agents at extinguishing flammable liquids because aerosol is rapidly entrained by combustion products. Fire suppression efficiency can be improved by optimizing the operating parameters of fire-extinguishing agents [18]. Various substances

can be added to water mist, and the resulting multiphase extinguishing agent can provide better fire suppression through bond cleavage in the flame. Koshiba et al. [19] established that surfactants are effective against fires, especially when oil fuels are involved. The foam blankets the oil surface, and surfactants emulsify it, thus slowing down the combustion process. Iron pentacarbonyl and ferrocene were shown to be good flame inhibitors [19,20]. However, the toxicity of these additives outbalances their flame suppression efficiency. At present, carbon dioxide is often used as a diluent of extinguishing agents to suppress flame combustion [17,21].

CO<sub>2</sub> hydrate is one of the multiphase composite extinguishing agents. Gas hydrates are solid crystalline compounds with gas and water molecules (the latter form a cage-like crystal lattice with hydrogen bonds) [22–24]. The equilibrium of the crystalline compound is provided by van der Waals forces at certain pressures and temperatures. An intense heat flux during combustion triggers the gas hydrate dissociation into ice and gas, as well as ice melting [25]. Due to ice crust melting, a water film is formed on the tablet surface and drains down on the fuel surface. As a result, both fuel and water evaporate [26,27]. CO<sub>2</sub> hydrates are widely used in several fields [28]: for sea water desalination [29], CO<sub>2</sub> storage [30–32], as well as cooling and production of carbonated solid foods [33–35]. Hydrates containing nonflammable gases, CO<sub>2</sub> in particular, can be used as fire suppressants because gas dissociation, ice melting, and water evaporation reduce the temperature in the flame zone. Nonflammable gases released from dissociating hydrates [36] prevent oxygen as well as pyrolysis and combustion products from entering the flame zone [37]. Presumably, the amount of hydrate required for fire suppression is much less than that of sprayed water, due to greater dissociation heat of hydrates and the release of nonflammable gases [37]. Fire extinguishing using powdered gas hydrate is understudied at this point [37,38]. Suppression of liquid methanol pool fires with ice, dry ice, and carbon dioxide hydrate powder with a particle diameter of less than 1 mm was compared in Ref. [37]. The critical mass of carbon dioxide hydrate required for the suppression of flame combustion was lower than that of ice. It was shown that the amount of CO<sub>2</sub> released during the suppression of flame combustion is lower when CO<sub>2</sub> hydrate is used as compared to dry ice, which testifies to the environmental friendliness of carbon dioxide hydrate as an extinguishing agent [37,38]. We studied the suppression of compartment fires involving solid materials with the help of carbon dioxide hydrates in our earlier papers. Experiments confirmed the high efficiency of CO<sub>2</sub> as an extinguishing agent compared to water, ice, and snow. The fire and explosion hazard of liquids is much higher than of solid substances in compartments, while the suppression of their combustion using gas hydrates has been largely overlooked. Studying the pool fire suppression using CO<sub>2</sub> hydrate is necessary and relevant, and yet the topic does not receive enough attention. This served as a motivation for this study.

The aim of this research was to experimentally determine the characteristics of heat and mass transfer, phase transitions, and chemical reactions during the interaction of CO<sub>2</sub> hydrate in the form of powder, granules, and tablets with burning liquid fuels and oil.

## 2. Experimental Technique

The experiments involved common fire-hazardous liquids: gasoline, kerosene, diesel fuel, alcohol, used motor oil, and petroleum. All the liquids but petroleum had certificates of conformity to ranks and were prepared in standardized conditions. The characteristics of such liquids comply with the quality standards of their producers (Table 1). We used two types of petroleum. Table 2 presents their main characteristics.

**Table 1.** Characteristics of flammable liquids and fuels in compliance with regulatory documents [39–42].

AI-92 gasoline	Octane number	91
	Lead content, g/dm <sup>3</sup>	0.010
	Manganese content, mg/dm <sup>3</sup>	18
	Oxidation stability of gasoline, min	360
	Existent gum content, mg/100 cm <sup>3</sup>	5
	Mass fraction of sulfur, %	0.05
TS-1 kerosene	Density at 20 °C, g/cm <sup>3</sup>	0.780
	Kinematic viscosity, mm <sup>2</sup> /s at 20 °C	1.3
	Lower heating value, kJ/kg	43120
	Mass fraction of total sulfur, %	0.2
Diesel fuel	Cetane number	45
	Kinematic viscosity, mm <sup>2</sup> /s at 20 °C	4
	Ash content, %	0.01
	Existent gum content, mg/100 cm <sup>3</sup> of fuel	30
Alcohol	Volume fraction of ethyl alcohol, %	96
	Oxidation test, min	15
	Mass concentration of dry residue, mg/dm <sup>3</sup>	2
	Mass concentration of sulfur, mg/dm <sup>3</sup>	no
Lukoil Genesis Armortech 5W30 used motor oil	Density at 15 °C, kg/m <sup>3</sup>	844.8
	Kinematic viscosity at 100 °C, mm <sup>2</sup> /s	9.7
	Viscosity index	173
	Sulfate ash content, %	1.05
	Flash temperature in open crucible, °C	223

**Table 2.** Experimentally obtained oil sample characteristics.

Name of Indicator	Unit of Measurement	Crude Oil	Separated Oil
		Test Result	Test Result
Mass fraction of water	wt%	2.37	no
Density at 15 °C	kg/m <sup>3</sup>	852.7	797.5
Density at 20 °C	kg/m <sup>3</sup>	849.2	792.5
Kinematic viscosity at 15 °C	mm <sup>2</sup> /s	–	4.391
Kinematic viscosity at 20 °C	mm <sup>2</sup> /s	7.567	1.741
Kinematic viscosity at 50 °C	mm <sup>2</sup> /s	3.943	–
Mass fraction of mechanical impurities	wt%	3.943	0.020
Freezing point	°C	–25.6	8

The following popular compositions were used as extinguishing agents for the containment and suppression of fires involving liquid fuels [14,15,43–45]: tap water, snow, and ice (for low-temperature climatic conditions where water supply is a problem), foaming agent emulsion (kinematic viscosity at 20 °C: no more than 200 mm<sup>2</sup>·s<sup>-1</sup>, pH at 20 °C: 6.5–10) with concentrations of 1% (density of the composition:  $\rho = 1068$  kg/m<sup>3</sup>) and 5% (density of the composition  $\rho = 1128$  kg/m<sup>3</sup>), and carbon dioxide hydrate powder and tablet.

Carbon dioxide is actively used in firefighting systems [17,46]. Fire containment and suppression happens fast because carbon dioxide does not contribute to the combustion front propagation or increase in the fire area but displaces the fire-supporting oxidizer. The main drawback of using CO<sub>2</sub> for fire suppression is the critical lack of oxygen, which is potentially hazardous to human life and health during evacuation. Carbon dioxide hydrate, however, contains water, so the influence of the above drawback is minimized. The water content in gas hydrate also contributes to the effective suppression of fires even in the case of multiphase reacting media. To enhance the role of water vapors in the presence of CO<sub>2</sub>, we used a hydrate with a limited content of gas in the crystal lattice. The carbon dioxide hydrate used in the experiments had the following component composition: 71–72% of water and 28–29% of CO<sub>2</sub> (powder); 75–76% of water and 24–25% of CO<sub>2</sub> (tablet); 80–81% of water and 19–20% of CO<sub>2</sub> (sphere). The particle size of CO<sub>2</sub> hydrate powder was 0.3–0.5 mm, which is a typical diameter of hydrate granules [47]. The CO<sub>2</sub> hydrate tablet was 20 mm in diameter and 5 mm in height. The initial mass of the sample tablet was 1.07 g, and the mass of the spherical hydrate sample was 1.42 g. The experiments with alternative extinguishing agents involved natural snow in the form of granules 1–3 mm in size. The masses of the extinguishing agents and flammable liquids used in the experiments were determined beforehand with the help of an AJH-620CE electric balance with an accuracy of  $\pm 0.001$  g.

Figure 1 schematically represents the setup used to experimentally study the fire containment and suppression. A flammable liquid sample (gasoline, kerosene, diesel fuel, alcohol, used motor oil, and petroleum) with a fixed initial mass was poured into a metal cup and then ignited by a gas burner (evenly across the entire surface). The exposure time of the laboratory-scale fire to the gas burner was about 2 s. Using a robotic arm, we supplied an extinguishing agent (snow, ice, water, foaming agent emulsion, and carbon dioxide hydrate in different forms) to the fire. The initial mass of the fuel was measured on an electronic balance. The temperature in the flame combustion zone (at different distances above the flammable liquid) was recorded by three type K chromel-alumel thermocouples (Owen DTPK1-0.5/2 021, type K, measurement range:  $-40$ – $1100$  °C, class 2 tolerance, response time no more than 3 s, accuracy  $\pm 2.5$  °C). The temperature readings were uploaded to the PC. The concentrations of gases emitted from the fuel combustion were measured using a Test 1 gas analyzer. The gas analyzer probe was introduced into the center of the cube through a special orifice on top. The combustion processes were recorded by a Phantom MIRO C110 camera with a frame rate of up to 1000 fps at a resolution of  $1280 \times 1280$  pix. The data obtained from the experiment were used to calculate the integral characteristics fire containment and suppression. The video recording and thermocouple measurements allowed us to track all the stages of fire suppression even during intense vaporization, smoke generation, and thermal decomposition of the materials accompanied by the formation of a gas-vapor mixture with high light absorption.

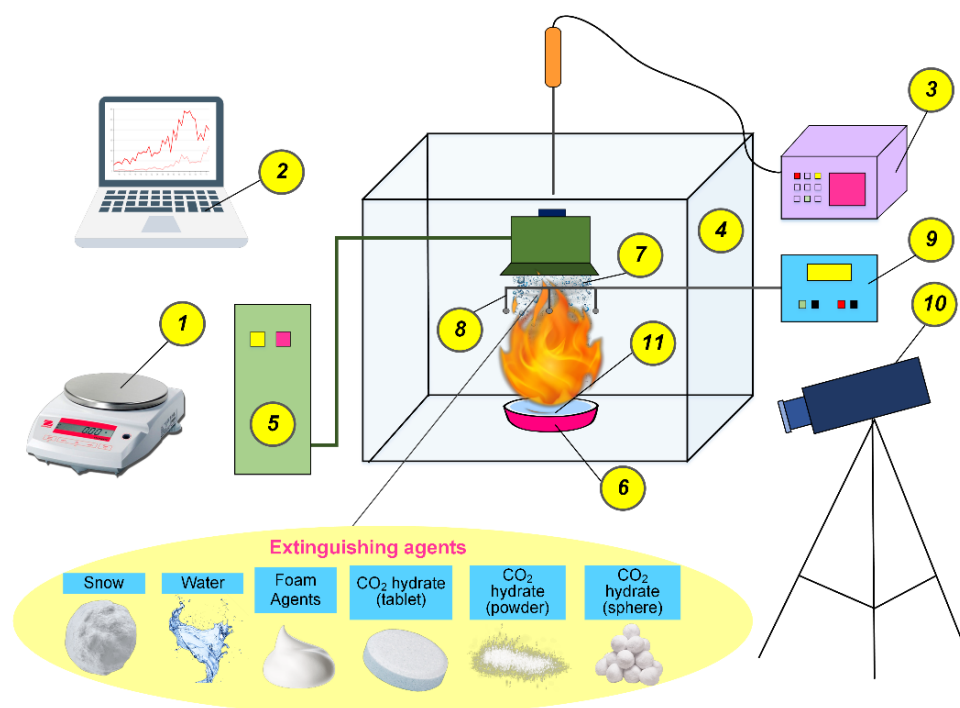


**Figure 1.** Scheme of setup: 1—electronic balance; 2—laptop; 3—gas analyzer; 4—transparent cube; 5—extinguishing agent feeder; 6—container with a burning liquid; 7—extinguishing agent; 8—thermocouple; 9—temperature transmitter; 10—camera; 11—flammable liquid.

### 3. Results and Discussion

#### 3.1. Patterns of Pool Fire Suppression

Figures 2–4 present typical images of pool fire suppression using carbon dioxide hydrate in the form of powder, tablets, and spheres. According to the data obtained, no more than 3–4 g of CO<sub>2</sub> hydrate is enough to suppress a flammable liquid pool fire with a volume of 3 mL. A further increase in the hydrate mass is unpractical and leads to the excessive carbon dioxide emission while the fire containment and suppression time remains almost the same. Thus, 1/1 is the optimal ratio of the burning liquid mass to the CO<sub>2</sub> hydrate powder mass for a small-volume pool fire.

Figure 2 shows that CO<sub>2</sub> hydrate powder enables faster gasoline fire suppression compared to hydrate tablets and spheres. The partial flame quenching with the help of carbon dioxide hydrate in the form of powder starts 2 s after the hydrate reaches the flame (Figure 2a). With tablets, however, the containment of flame combustion starts 15 s after the samples reach the fire (Figure 2b), and with spherical samples, it starts after 12 s (Figure 2c). This is related to the coverage of the fire by the extinguishing agent (carbon dioxide hydrate sample). Hydrate powder covers almost the entire combustion zone, whereas hydrate tablets and spheres act locally on the flame. Different flame quenching times by CO<sub>2</sub> hydrate in the form of tablets and spheres stem from the same reasons. Artificial spherical hydrate granules provide the smallest coverage of the fire (and hence the smallest contact area) compared to other forms (tablets and powder). Supplementary Materials Videos S1 and S2 present the video clips of gasoline fire suppression using hydrate powder with a mass of 3 and 4 g, respectively, and Supplementary Material Video S3 presents the videograms of using two hydrate tablets. The analysis of the footage indicates that granules that are evenly distributed over the combustion zone are more effective than tablets. The greater the mass of the powder sample, the less time is needed for fire suppression.



**Figure 2.** Images of gasoline fire suppression ( $V_0 \approx 3$  mL) with the help of carbon dioxide hydrate in the forms of (a) powder,  $m_g \approx 4$  g; (b) tablets,  $m_g \approx 1.07$  g; (c) spheres,  $m_g \approx 1.42$  g ( $d_f \approx 65$  mm,  $S_f \approx 33$  cm<sup>2</sup>).

The following patterns were identified on the images of diesel fire suppression (Figure 3). When in contact with the CO<sub>2</sub> hydrate powder, the flame was partially quenched 2 s after the powder reached the seat of fire, which is similar to the gasoline fire suppression (Figure 3a). When diesel fuel fire is suppressed by a carbon dioxide hydrate tablet, suppression takes longer (11 s) than in the case of spherical hydrate samples (5 s). This happens because the diesel fuel combustion temperature (about 1100 °C) is lower than the gasoline combustion temperature (about 1300–1400 °C). Therefore, the carbon dioxide hydrate spheres suppress a diesel fuel fire 2.5–3 times faster than a gasoline fire. Typical video clips showing the interactive diesel fuel fire suppression are shown in Supplementary Material Video S4.



**Figure 3.** Images of Diesel fuel fire suppression ( $V_0 \approx 3$  mL) with the help of carbon dioxide hydrate in the forms of (a) powder,  $m_g \approx 4$  g; (b) tablets,  $m_g \approx 1.07$  g; (c) spheres,  $m_g \approx 1.42$  g ( $d_f \approx 65$  mm,  $S_f \approx 33$  cm<sup>2</sup>).

Figure 4 presents the experimental images of kerosene, motor oil, and petroleum fire suppression using CO<sub>2</sub> hydrate powder as an extinguishing agent. In the case of kerosene, oil, and petroleum combustion, the flame is quenched within 1–2 s after the hydrate powder is poured into the combustion zone. A kerosene fire is almost completely suppressed 2 s after the beginning of powder interaction with the source of fire. The carbon dioxide hydrate powder covers the entire combustion area, thus blanketing the fire, which leads to complete fire extinction. As a result of the increase in the temperature transferred from the flame zone to the hydrate sample, a well-known phenomenon occurs: self-preservation of the gas hydrate. The CO<sub>2</sub> hydrate powder turns into an ice-like structure after extinguishing the fire, which can be clearly seen in Figure 4a. Hydrate pores

are blocked by the frozen water particles, preventing the further release of carbon dioxide. This effect reduces the  $\text{CO}_2$  concentrations in the fire suppression zone. The dynamics of the oil, kerosene, and petroleum fire suppression processes are comparable. In particular, Supplementary Material Video S5 shows typical video clips of the experiments with an oil fire. It is established that when the burning motor oil interacts with the  $\text{CO}_2$  hydrate powder, the resulting gas–vapor mixture begins to burn actively, followed by pulsating burnout due to the interaction between oil and water particles contained in the hydrate sample (Figure 4b). The flame is quenched after 1–3 s. The breakup of droplets and volatile oil combustion products is also observed (Figure 4b). Bouncing occurs because oil has a higher boiling temperature than water does. Thus, water particles formed as a result of the carbon dioxide hydrate dissociation evaporate rapidly when in contact with burning oil. The resulting vapor flow destroys the oil film, followed by a pulsing burst of droplets filled with bubbles. Similar droplet breakup is observed when a crude oil pool fire is extinguished by hydrate powder (Figure 4c).



**Figure 4.** Images of flammable liquid fire suppression ( $V_0 \approx 3 \text{ mL}$ ) by carbon dioxide hydrate powder,  $m_g \approx 4 \text{ g}$ : (a) kerosene; (b) motor oil; (c) crude oil ( $d_f \approx 65 \text{ mm}$ ,  $S_f \approx 33 \text{ cm}^2$ ).

The conditions of hydrate distribution over the surface of the burning liquid in the form of a layer of granules play an important role. It is shown that CO<sub>2</sub> hydrate spheres and tablets effectively contain and suppress combustion only in the case of small areas of the reacting substances and confined volumes, i.e., without oxygen inflow. Granulated carbon dioxide hydrate is more versatile in this respect: it can effectively cover quite a large surface area of the burning material. In this case, the CO<sub>2</sub> release from the volume of the hydrate will be rather significant and fast. A lot of the energy of the fire is also spent on heating ice and water as well as on their melting and evaporation. The main factors that lead to the suppression of fires involving flammable liquids by CO<sub>2</sub> hydrate are as follows: rapid decrease in the flammable liquid temperature; access of granulated powder to the lower levels of the fire; oxygen depletion due to the release of a large amount of carbon dioxide. The conditions in which each of the mechanisms under study dominates can be ensured by the proper supply of gas hydrate to the combustion zone or ahead of the combustion front. Supplementary Material Video S6 shows a video clip of oil fire suppression using two gas hydrate spheres where the above effects are demonstrated. Of all the liquids under study, the fastest and least expensive fire suppression was observed in the experiments with alcohol. Supplementary Material Video S7 shows a typical video clip for this case.

### 3.2. Quantitative Characteristics of Fire Containment and Suppression

Figures 5–8 present the fire extinction time (including fire containment and subsequent suppression) obtained in the experiments. We studied the fire evolution when no extinguishing agents were used and when the fire was suppressed by water aerosol, foaming agent emulsion, snow, ice, and CO<sub>2</sub> hydrate samples in the form of powder, tablets, and spheres. The principal physical differences between the conditions of fire suppression using different extinguishing agents were observed quite consistently. When CO<sub>2</sub> hydrate with  $m_g \approx 1$  g was used, the flame quenching time was 60% shorter. The use of the CO<sub>2</sub> hydrate powder as an extinguishing agent for gasoline fire reduces the flame quenching time almost by half (from  $t \approx 38$  s to  $t \approx 24$  s), with an increase in the mass of carbon dioxide hydrate from  $m_g \approx 1$  g to  $m_g \approx 2$  g (Figure 5a). It was established that a two-times-larger volume of the flammable liquid would require a 4.5 increase in the mass of the extinguishing agent to ensure the identical flame quenching time. This happens because the larger the combustion area, the greater volume of powder is required to cover the fire for its containment and suppression.

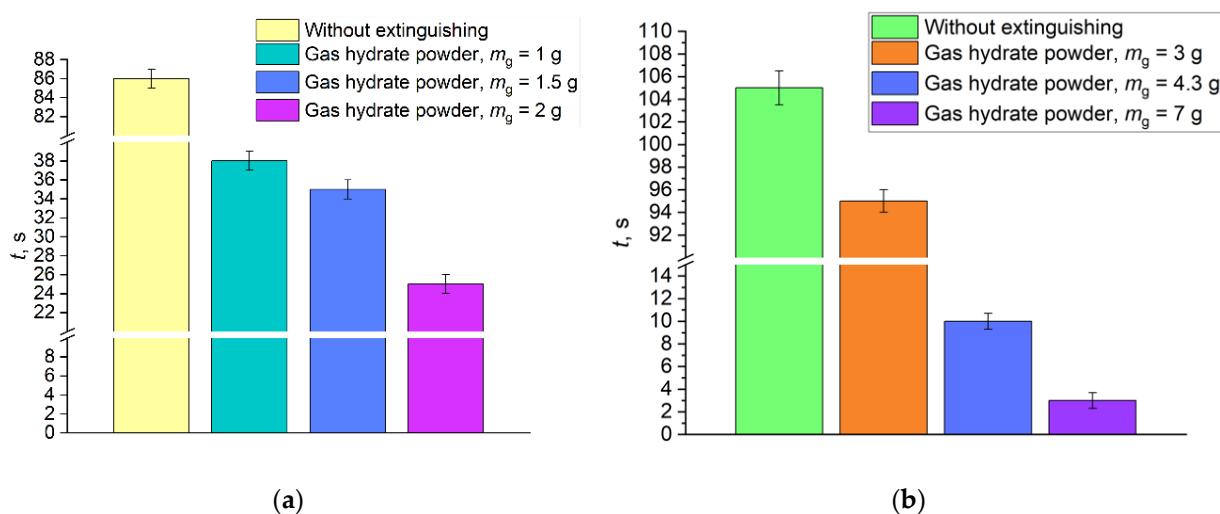


**Figure 5.** Extinction times of gasoline with varying initial volume ( $V_0$ ) burning when no extinguishing agents were used and when in contact with CO<sub>2</sub> hydrate powder with varying initial mass  $m_g$ : (a)  $V_0 \approx 3$  mL; (b)  $V_0 \approx 6$  mL.

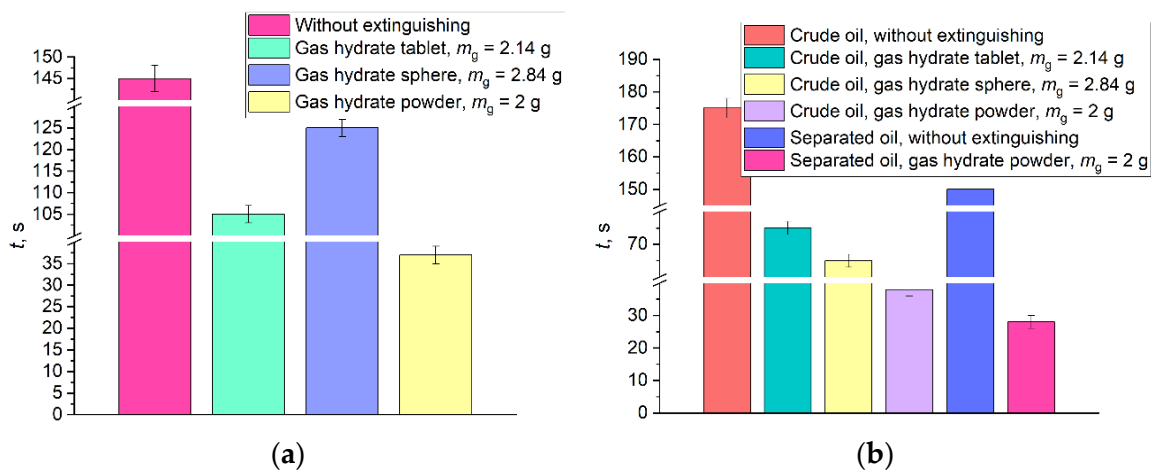


**Figure 6.** Extinction times of (a) diesel fuel ( $V_0 \approx 3$  mL) and (b) petroleum ( $V_0 \approx 3$  mL) pool fires without extinguishing and when suppressed by CO<sub>2</sub> hydrate in the form of powder, tablets, and spheres with varying initial mass  $m_g$ .

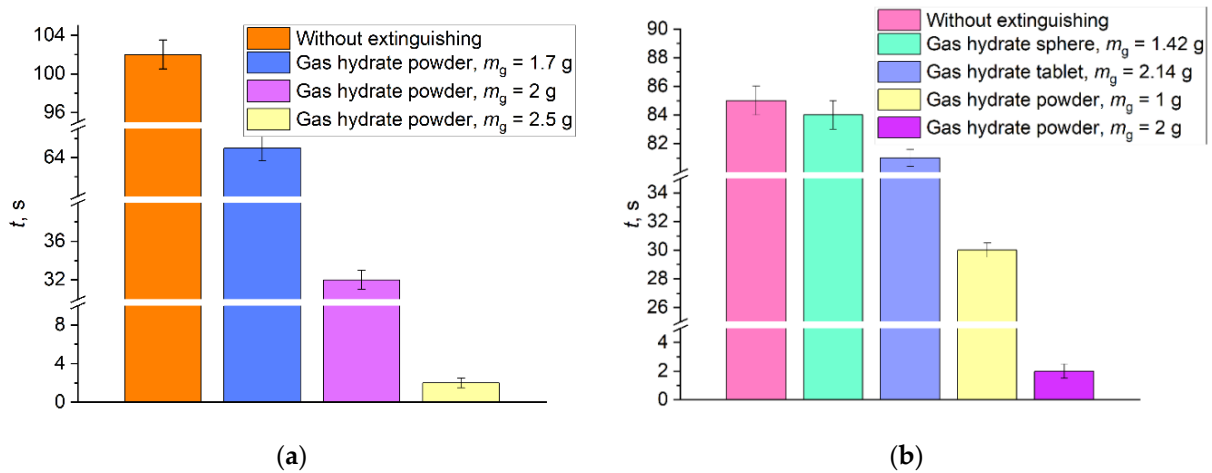


**Figure 7.** Extinction times of (a) kerosene ( $V_0 \approx 3$  mL) and (b) alcohol ( $V_0 \approx 3$  mL) pool fires without extinguishing and when suppressed by CO<sub>2</sub> hydrate in the form of powder, tablets, and spheres with varying initial mass  $m_g$ .

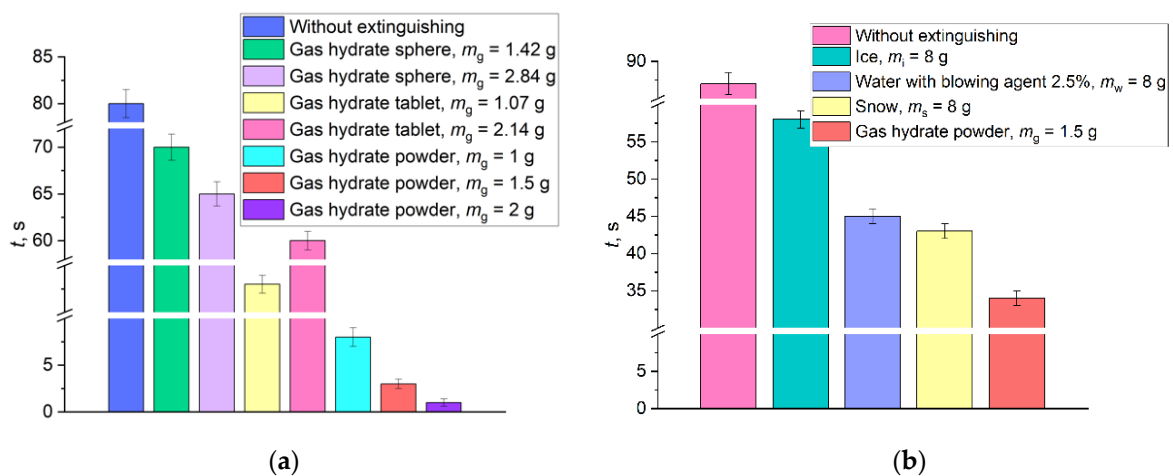


**Figure 8.** Extinction times of a gasoline pool fire ( $V_0 \approx 3$  mL) without extinguishing and when suppressed by (a) CO<sub>2</sub> hydrate in the form of powder, tablets, and spheres with varying initial mass  $m_g$ , and (b) ice and water with 2.5% of foaming agent, snow, and CO<sub>2</sub> hydrate powder.

We compared the flame extinction time for diesel fuel of the same volume  $V_0 \approx 3$  mL exposed to CO<sub>2</sub> hydrate in different forms (tablets, spheres, and powder) to find that powder was by far the most effective form of hydrate for suppressing the combustion of the liquids under study. With the mass of the extinguishing agent samples being about equal, the flame extinction time was almost four times shorter when CO<sub>2</sub> hydrate powder was applied (Figure 6a). Crude oil without exposure to extinguishing agents showed the longest fire extinction time: 175 s (Figure 6b). The use of carbon dioxide hydrate in the powder form for extinguishing crude and separated oil reduced the flame extinction time by 60–96%.

Figure 7 shows the flame extinction times of burning kerosene (Figure 7a) and alcohol (Figure 7b) with and without extinguishing agents being used in the process. The use of CO<sub>2</sub> hydrate powder with an initial mass of 1.7–2.5 g can reduce the kerosene flame extinction time by 37–97%. Alcohol fire with an initial volume of 3 mL was extinguished using carbon dioxide hydrate in the form of a sphere, tablets, and powder (Figure 7b). The most effective extinguishing agent in terms of the flame extinction time was the CO<sub>2</sub> hydrate powder, with an initial mass of 2 g due to its full coverage of the fire, and thus depriving the fire of the oxidizer.

The minimum flame extinction time (30 s) is observed when a gasoline fire is suppressed by 2 g of carbon dioxide powder (Figure 8a). Fire suppression with a single CO<sub>2</sub> sphere provides a 14% shorter extinction time compared to the case when no extinguishing agents are used and using a twin CO<sub>2</sub> sphere ensures a 20% reduction in the extinction time. A carbon dioxide tablet shortens the gasoline fire extinction time by half. Using gas hydrate powder as an extinguishing agent for gasoline fire suppression reduces the flame extinction time by 58% compared to ice, by 75% compared to a foaming agent, and by 79% compared to snow (Figure 8b). We have arranged the extinguishing agents under study in the order of growing effectiveness at reducing the gasoline fire ( $V_0 \approx 3$  mL) extinction time: ice, foaming agent emulsion, water, snow, and, finally, CO<sub>2</sub> hydrate powder ( $m_g \approx 1.5$  g). Carbon dioxide hydrate powder was highly effective at suppressing the flame combustion and quickly reduced the temperature in the combustion zone because the dissociation and melting time of a gas hydrate particle was as short as 0.1–1 s. This time was enough for most of the granules to reach the flame base. The free-fall time of powder particles was less than 0.1 s. As a result, components of the inert mixture—carbon dioxide and water vapors—were present in high concentrations throughout the flammable liquid. The temperature in the fire source decreased rapidly due to the dissociation heat of the gas hydrate, ice melting, and water evaporation, as well as due to the low initial temperature of the granules (about  $-30$  °C).

The fire containment and suppression mechanism of CO<sub>2</sub> hydrate powder is based on cooling the fire source. Hydrate granules formed a film on the surface of the burning liquid during the heat exchange with it. Due to high heat capacity of water and high vaporization heat, a significant heat removal was observed from the surface to the depth of the hydrate, which catalyzed the CO<sub>2</sub> release. The hydrate layer became heterogeneous: it was a composition of hydrate, ice, water, as well as vapor and gas bubbles. Such structures are more effective for heat exchange than homogeneous ones. Snow and ice powder supplied to the surface of the flammable liquid also provided denser coverage of the surface, but the presence of vaporization centers in the hydrates in the form of ice particles, water droplets, and gas bubbles intensified the cooling of the fire source. Fire suppression by water/foaming agent emulsion has shown that water spray coming from an atomizer only suppresses the flame at the upper layer of the fire. Due to high temperatures in the flame zone, water emulsion droplets evaporate too rapidly to penetrate and reach the deep layers of flame. Free gravitational convection carries the water vapor upwards, excluding the access of both vapor and small water droplets to the lower part of the combustion zone. Another important benefit of carbon dioxide hydrates as fire suppressants is the active displacement of the oxidizer from the combustion zone. This does not only slow down the

oxidizing reactions but also starts the reactions inhibiting the growth of the concentrations of harmful emissions typical of fire suppression with water at a certain stage.

Fires involving flammable liquids in industrial buildings and warehouses emit large amounts of harmful anthropogenic gases that pose a threat to human lives and health. It is important to evaluate the effect of water contained in the gas hydrate on the concentration of harmful emissions. Figures 9–11 show the concentrations of the main gases emitted from the combustion and suppression of a fire involving flammable liquids with variable extinguishing agents. According to the data obtained, the maximum CO<sub>2</sub> concentrations correspond to the combustion of gasoline, kerosene, and alcohol without extinguishing and equaled 2.7–2.9 vol%. The use of any of the extinguishing agents under study provided a 4% to 40% decrease in CO<sub>2</sub> emissions into the atmosphere. The lowest CO<sub>2</sub> concentrations from the suppression of a flammable liquid fire were observed when using water and carbon dioxide hydrate powder with a mass of no more than 1.5 g (Figure 9a). The use of CO<sub>2</sub> hydrate triggered two main mechanisms of fire containment. The temperature in the gas phase decreased due to the gas hydrate dissociation, ice shell melting, and water evaporation. The inert gas rapidly released from the hydrate and displaced the oxygen from the combustion zone, thus inhibiting the oxidation of flammable liquids. A decrease in the production rate of H, O, and OH radicals in the reaction zone led to a rapid deceleration of the combustion front propagation and subsequent flame quenching. When 2 g of CO<sub>2</sub> hydrate was used for suppressing a 3 mL gasoline fire, the concentrations of CO<sub>2</sub> emitted from the suppression increased due to the gas hydrate dissociation. In the course of dissociation, while the hydrate mass increased and the volume of the flammable liquid remained constant, more hydrate particles dissociated into ice and carbon dioxide, whose concentration began to grow. The interaction between the carbon monoxide produced from gasoline combustion and water vapor released from the dissociated hydrate intensified the gas–water shift reaction ( $\text{CO} + \text{H}_2\text{O} \leftrightarrow \text{CO}_2 + \text{H}_2$ ). Due to this reaction, the CO concentration decreased significantly during the flame suppression by carbon dioxide hydrate (Figure 9b), while the CO<sub>2</sub> concentration increased because some of the carbon monoxide converted to carbon dioxide.

The maximum CO concentrations were observed when an alcohol fire was suppressed by CO<sub>2</sub> hydrate powder (Figure 10b). The use of the latter reduced the CO emission by half, partly because of the gas–water shift reaction. The extinguishing agents under study, arranged from less effective to more effective at reducing the carbon monoxide emissions, are as follows: snow, foaming agent emulsion, water, ice, and, finally, CO<sub>2</sub> hydrate powder ( $m_g \approx 2$  g). It is noteworthy that the CO<sub>2</sub> hydrate powder with  $m_g = 1$ –1.5 g is enough for gasoline fire suppression ( $V_0 \approx 3$  mL) but not enough for a significant reduction in the CO emissions. A similar trend is observed in the case of petroleum fire suppression. The use of CO<sub>2</sub> hydrate powder as an extinguishing agent reduces the CO<sub>2</sub> and CO concentrations by 3% (Figure 11). Due to the content of water in separated oil, water vapors released during combustion reacted with carbon monoxide to form greater CO<sub>2</sub> concentrations as compared to crude oil.

Figure 12 shows the temperature trends illustrating the flame temperature variation dynamics (AI-92 gasoline) without extinguishing and when using CO<sub>2</sub> hydrate powder ( $m_g = 0.6$ –2 g). The flame temperature was measured by chromel–alumel thermocouples. The thermocouple junctions (Figure 12) were located at different distances from the flammable liquid surface: T#1—10 mm; T#2—30 mm; T#3—50 mm. We used the following notations in Figure 12:  $t_b$  is the fire extinction time;  $t^*$  is the moment of the extinguishing agent supply;  $t_e$  is the time from ignition to extinction. According to Figure 12, when fire suppression is not provided, a short-term temperature decrease (down to 70–300 °C) is observed at the beginning of the experiment when an extinguishing agent is supplied; after that, the flame temperature goes back to its initial values (500–650 °C). The experiments also established (Figure 12) that the necessary mass of the CO<sub>2</sub> hydrate powder for the suppression of a laboratory-scale gasoline fire is 1.5–2 g, which is equivalent to the discharge density  $\zeta = 0.75$ –1 kg/m<sup>2</sup>. With a mass of the hydrate powder of about 1 g, the suppression

was successful in about 50% of cases. No fire suppression was observed when the mass was 0.6 g.

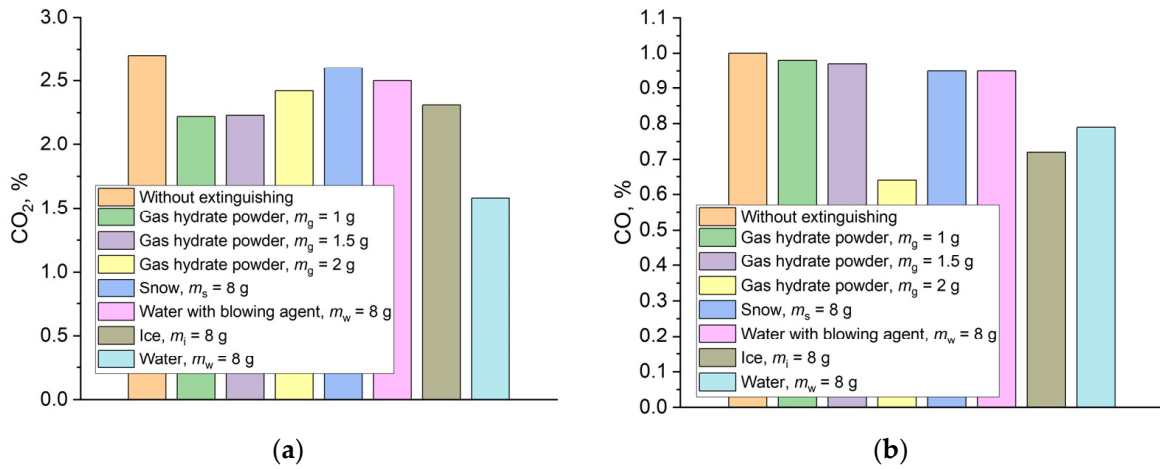


Figure 9. Concentrations of CO<sub>2</sub> (a) and CO (b) from the suppression of a gasoline fire ( $V_0 \approx 3$  mL) by different extinguishing agents.

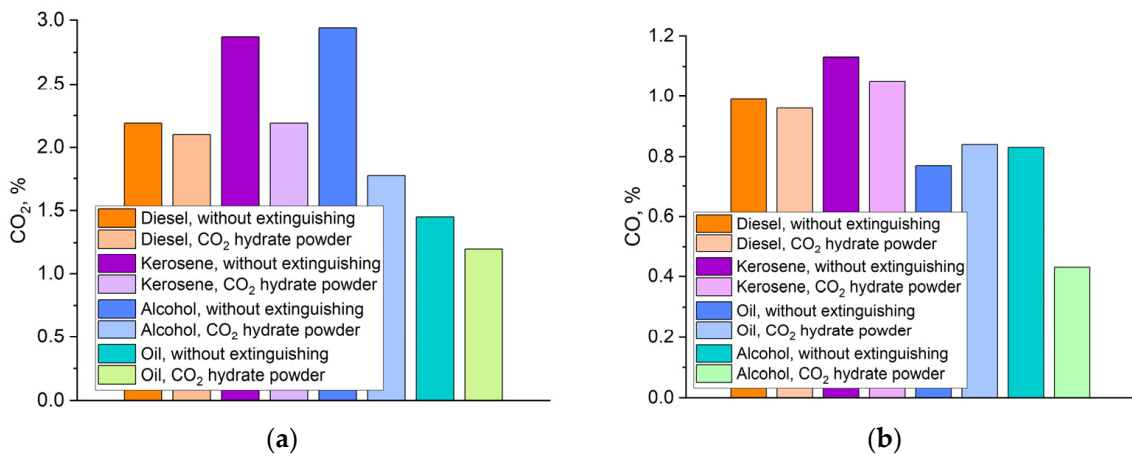


Figure 10. Concentrations of CO<sub>2</sub> (a) and CO (b) from the suppression of flammable liquids (diesel fuel, kerosene, oil, and alcohol) by CO<sub>2</sub> hydrate.

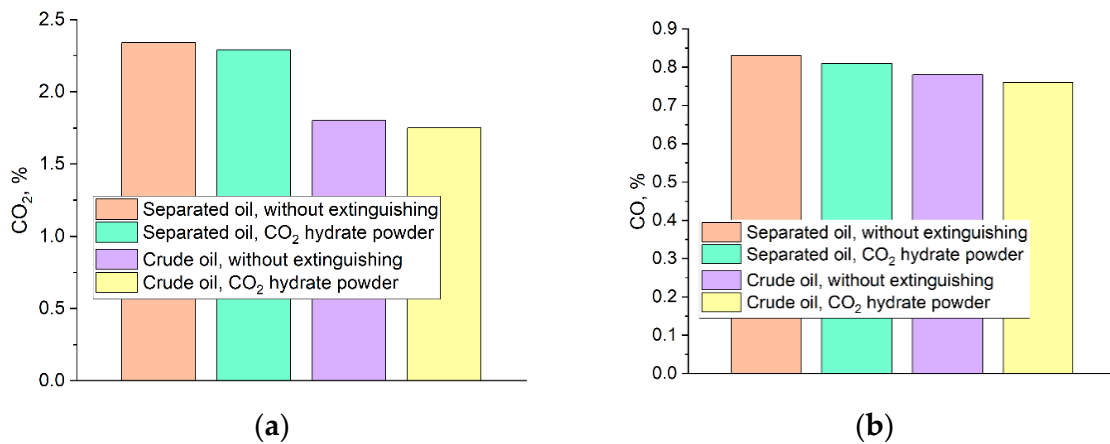
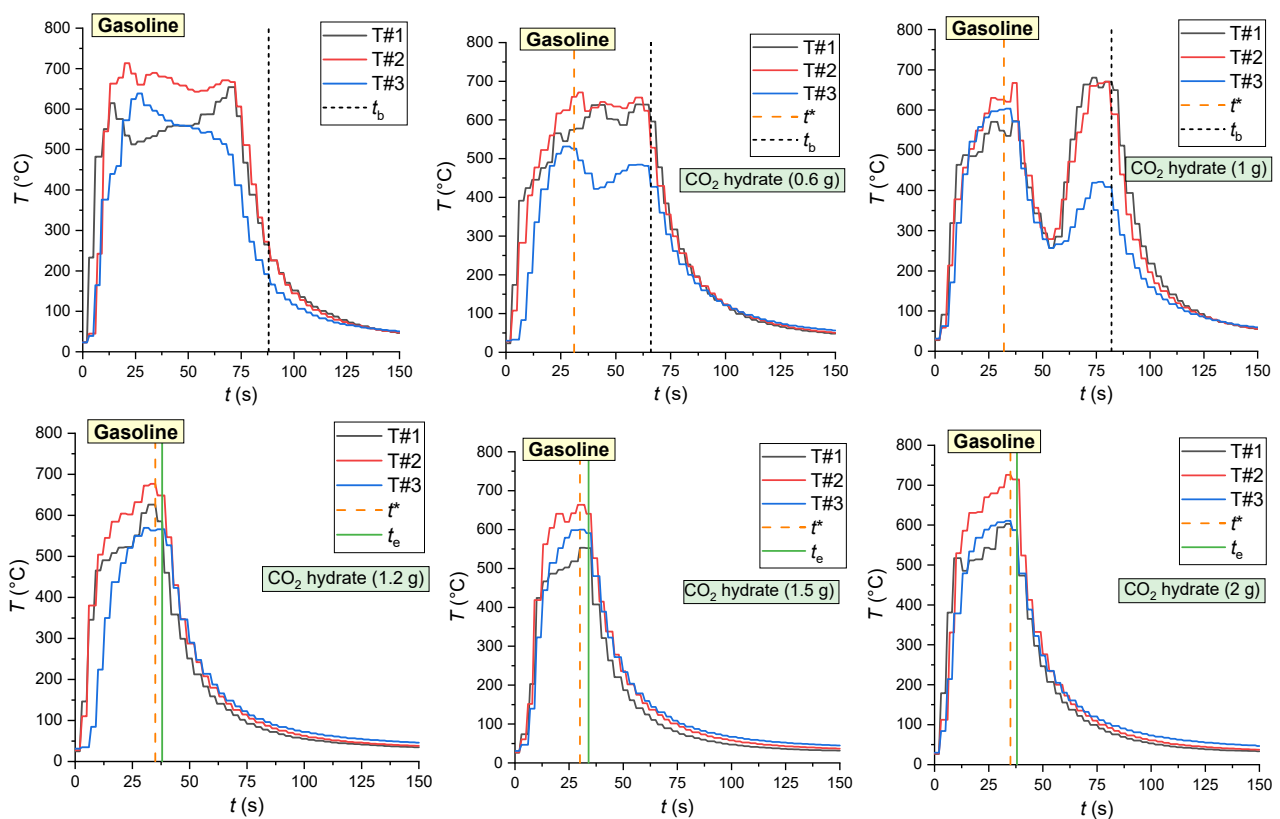
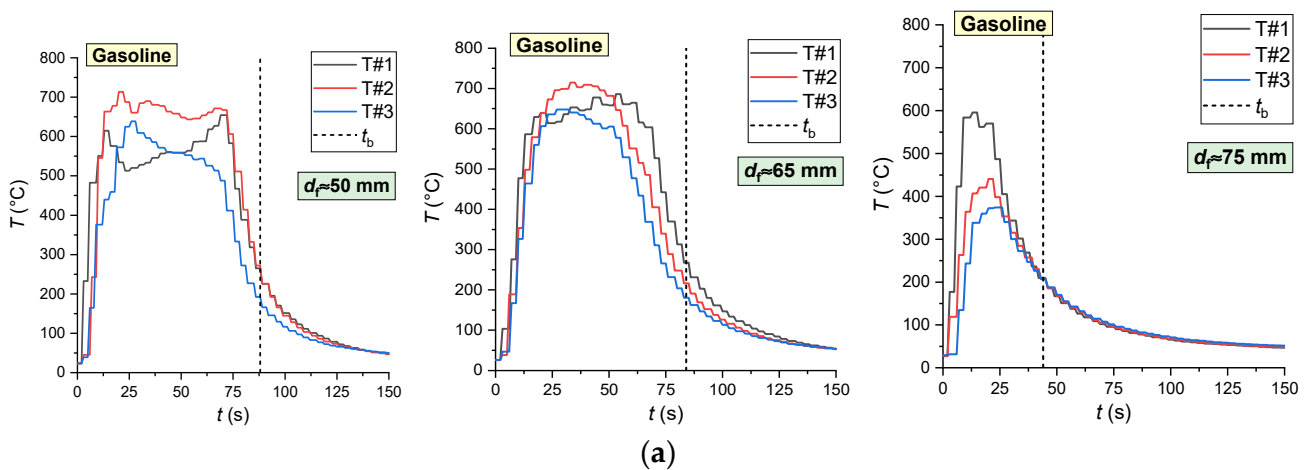


Figure 11. Concentrations of CO<sub>2</sub> (a) and CO (b) released during the suppression of crude and separated oil fire by CO<sub>2</sub> hydrate.



**Figure 12.** Flame temperature variation dynamics (gasoline,  $V_0 \approx 3$  mL,  $d_f \approx 50$  mm,  $S_f \approx 20$  cm<sup>2</sup>) without extinguishing and when using CO<sub>2</sub> hydrate powder ( $m_g = 0.6$ – $2$  g).

Figure 13 presents the temperature trends illustrating the flame temperature variation dynamics for laboratory-scale pool fires of different diameters ( $d_f = 50$ – $75$  mm) consisting of gasoline ( $V_0 \approx 3$  mL) and burning without extinguishing and when suppressed by CO<sub>2</sub> hydrate powder. The trends were obtained using thermocouple measurement. It was established (Figure 13a) that with  $V_0 \approx \text{const}$ , an increase in the fire surface area in the range of  $S_f = 20$ – $45$  cm<sup>2</sup> leads to a nonlinear decrease in the flammable liquid fire extinction time from 88 s to 44 s (because it burns evenly at the same rate across the entire fire surface area). According to the generalized data (Figure 13b), the minimum required discharge density of the CO<sub>2</sub> hydrate per unit area of the flammable liquid surface must be  $\zeta = 0.5$ – $0.6$  kg/m<sup>2</sup>.



**Figure 13.** Cont.

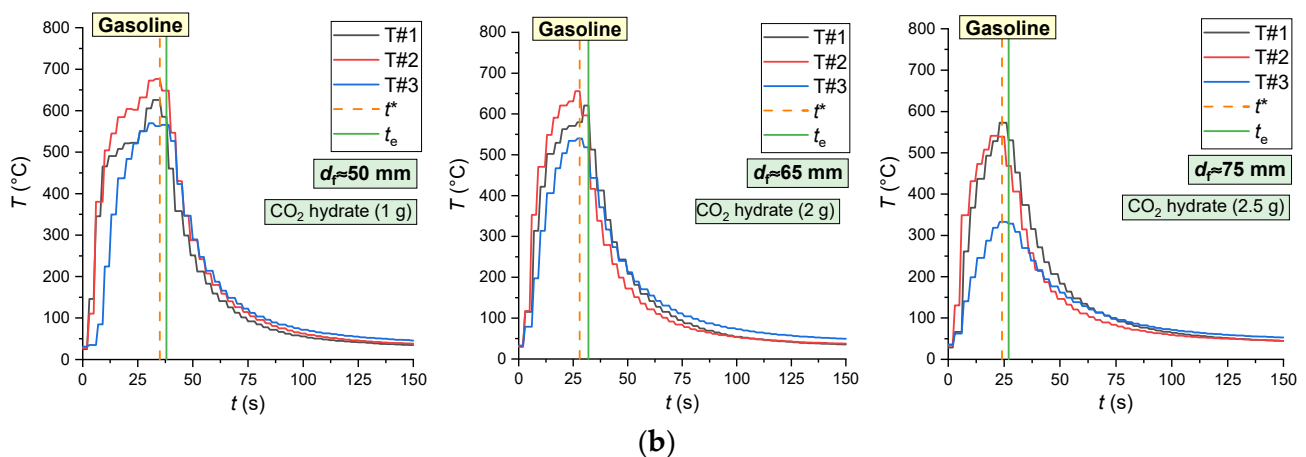
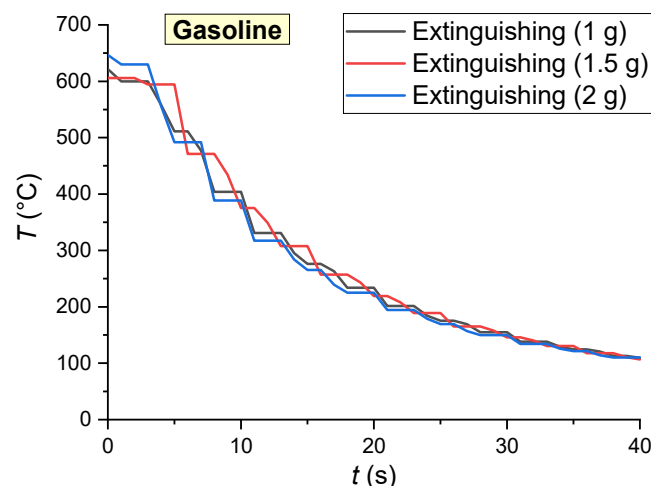


**Figure 13.** Flame temperature variation dynamics for laboratory-scale pool fires of different diameters ( $d_f = 50\text{--}75$  mm) consisting of gasoline ( $V_0 \approx 3$  mL) and burning without extinguishing (a) and when exposed to  $\text{CO}_2$  hydrate powder (b).

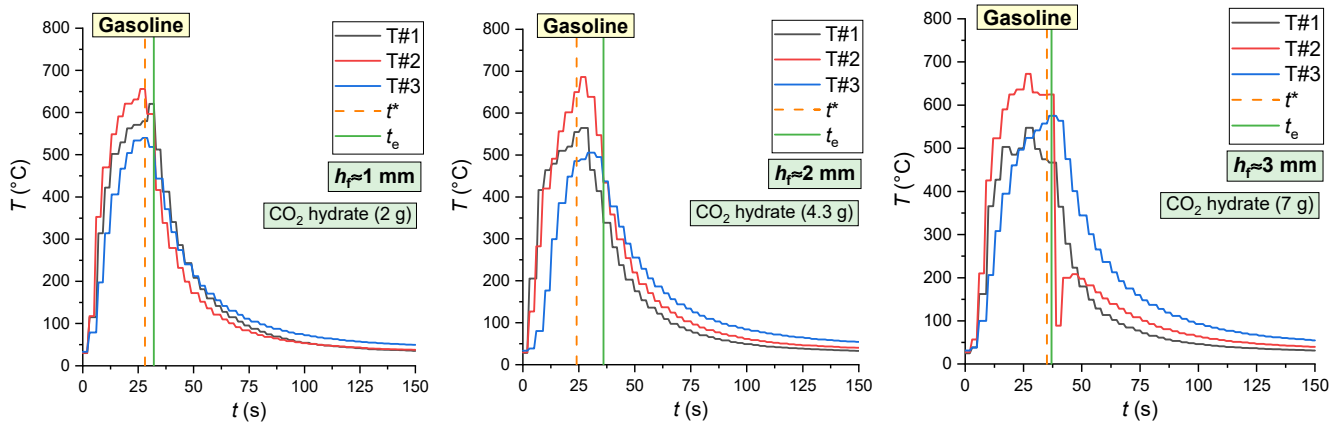
Figure 14 presents combined experimental trends (arithmetic mean of the readings from the three thermocouples in the experiment) of the successful suppression of a laboratory-scale gasoline fire, illustrating the flame temperature variation dynamics immediately after the discharge of the extinguishing agent— $\text{CO}_2$  hydrate powder—onto the fire. The time interval ( $\Delta t_e$ ) from the moment of the extinguishing agent's discharge to the moment of fire extinction was 3–4 s in all three cases. Figure 14 shows that the temperature variation dynamics are almost identical.

Figure 15 presents the temperature trends illustrating the flame temperature variation dynamics of a laboratory-scale gasoline fire exposed to an extinguishing agent— $\text{CO}_2$  hydrate powder—with varying thickness of the fuel film (layer).

The experiments established (Figure 15) that the mass of the  $\text{CO}_2$  hydrate powder (and, hence, its discharge density) required for the fire extinction increases nonlinearly with an increase in the fuel (gasoline) layer thickness. An approximation,  $\zeta = f(h_f)$ , was constructed using the experimental findings (Figure 16).



**Figure 14.** Combined experimental trends of the successful suppression of a laboratory-scale gasoline fire ( $V_0 \approx 3$  mL,  $d_f \approx 50$  mm,  $S_f \approx 20$  cm<sup>2</sup>) illustrating the flame temperature variation dynamics immediately after the discharge of the extinguishing agent— $\text{CO}_2$  hydrate powder—onto the fire.



**Figure 15.** Flame temperature variation dynamics (gasoline,  $V_0 \approx 9$  mL,  $d_f \approx 65$  mm,  $S_f \approx 33$  cm<sup>2</sup>) of laboratory-scale fires suppressed by CO<sub>2</sub> hydrate powder with varying thickness of the fuel film (layer).

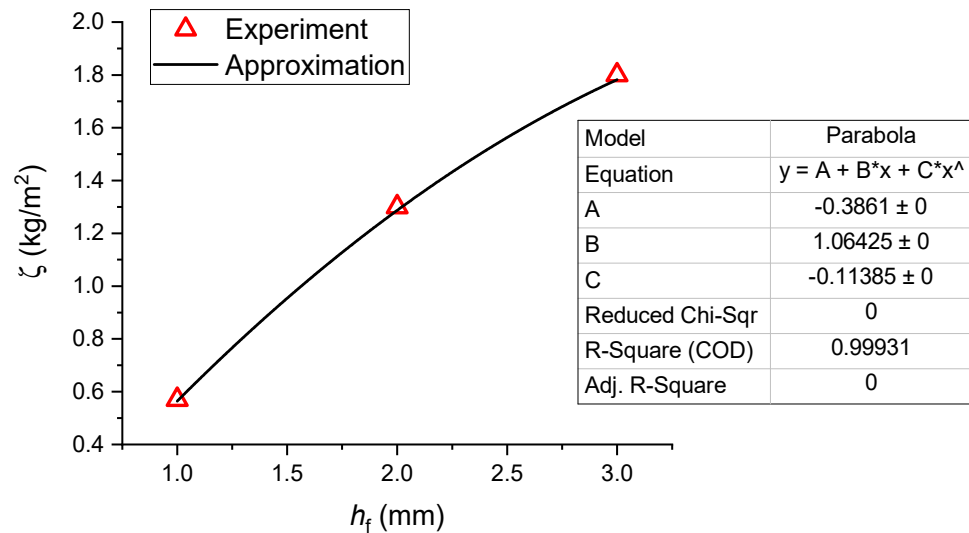


**Figure 16.** CO<sub>2</sub> hydrate powder discharge density per unit area of the flammable liquid versus the thickness of the liquid layer necessary and sufficient for the suppression of a laboratory-scale class B fire.

Figure 17 shows the temperature trends illustrating the flame temperature variation dynamics of a laboratory-scale gasoline fire without extinguishing and when suppressed by CO<sub>2</sub> hydrate powder ( $m_g = 0.6$ – $2$  g). It was established (Figure 17) that, almost irrespective of the type of the flammable liquid, the necessary and sufficient mass of the CO<sub>2</sub> hydrate powder for the suppression of a pool fire is  $m_g = 1.5$ – $2.5$  g, which is equivalent to the discharge density  $\zeta = 0.75$ – $1.25$  kg/m<sup>2</sup>.

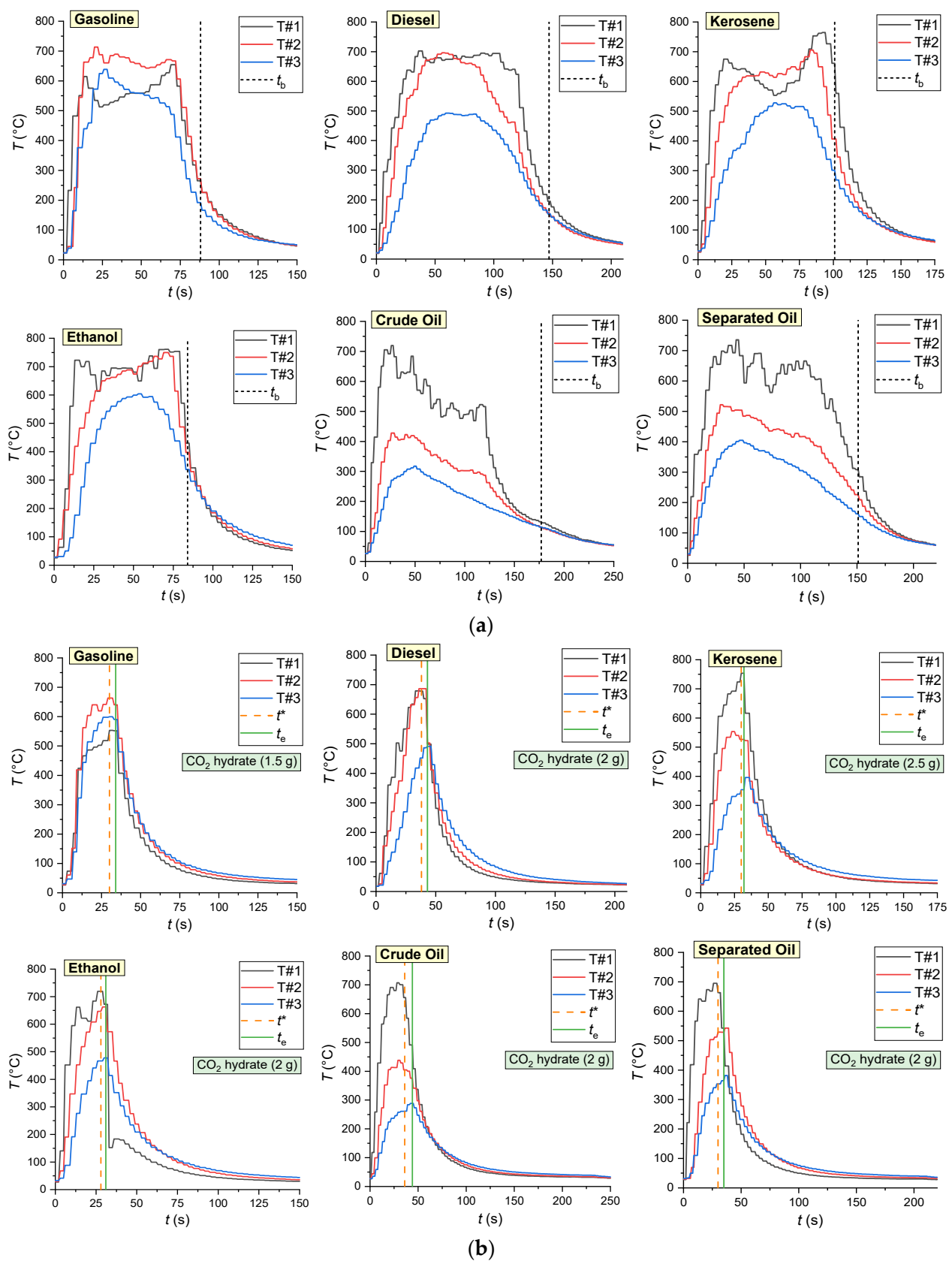


**Figure 17.** Flame temperature variation dynamics of laboratory-scale fires involving different flammable liquids ( $V_0 \approx 3$  mL,  $d_f \approx 50$  mm,  $S_f \approx 20$  cm<sup>2</sup>) without extinguishing (a) and when suppressed by CO<sub>2</sub> hydrate powder (b).

The analysis of temperature trends and other findings (Figures 12–17) led us to conclude that the suppression of a class B fire (irrespective of the type of flammable liquid involved and the fire surface area) with a fuel film thickness under 2 mm will require a CO<sub>2</sub> hydrate powder discharge density of at least 1.3 kg/m<sup>2</sup>. Given the suppressant pouring time into the fire, the laboratory-scale fire extinction will require a specific discharge density of at least  $\zeta_0 \approx 0.2$  kg/(m<sup>2</sup>·s) (when suppressing a similar fire with a coarse water aerosol, the value is  $\zeta_0 \approx 1.5$  kg/(m<sup>2</sup>·s)). With an increase in the flammable liquid film thickness (Figure 16), the necessary specific discharge density of the CO<sub>2</sub> hydrate increases:  $\zeta_0 \approx 0.3$  kg/(m<sup>2</sup>·s) for  $h_f \approx 2$  mm and  $\zeta_0 \approx 0.5$  kg/(m<sup>2</sup>·s) for  $h_f \approx 3$  mm. It is shown that the CO<sub>2</sub> hydrate powder discharge density necessary and sufficient for the suppression of a laboratory-scale class B fire increases nonlinearly with an increase in the fuel layer (an approximation was obtained to predict the values for different applications). Thus, the use of gas hydrates as extinguishing agents combines the benefits of conventional firefighting systems while eliminating their drawbacks. The research has shown the advantages of carbon dioxide hydrates for flammable liquid fire suppression. A high-potential objective for further research will be to extend the research findings to the real industrial environment as well as to search for the effective hydrate discharge systems for fire containment and suppression. Gas hydrate powder can be used as a component of a control line. The experiments imitating the operation of a control line against a kerosene fire showed that the flame does not transfer over the line if the line fully separates the fuel that is burning from the one that is not. The rapid in-blow of dissociation products and water vapors blocks the burning fuel. However, if the line has gaps or if the fuel burnout time is longer than the carbon dioxide dissociation time, the combustion front will burn through the control line (Supplementary Material H).

#### 4. Effective Conditions for Extinguishing Burning Liquids during the Dissociation of Carbon Dioxide Hydrate

The dissociation of gas hydrates at temperatures below the ice melting point is much more difficult to reproduce by mathematical modeling than at  $T > 0$  °C. A porous ice shell is formed at low temperatures. The resistance to gas filtration through pores increases sharply due to the partial closing of pores in the annealing temperature window, and the dissociation rate decreases as a result [48]. This phenomenon is known as self-preservation [49,50]. The influence of the key parameters (ice porosity, heat exchange, particle size) on the gas hydrate dissociation rate is considered in Ref. [51]. Large amounts of water vapor are produced from the combustion of gas hydrates, which can lead to a decrease in the combustion temperature and overall fire suppression [52,53]. The modeling of combustion during the gas hydrate dissociation is considered by Misyura and Donskoy [54]. Equation (1) can be used for modeling the gas hydrate dissociation at low temperatures, controlling for ice porosity, dissociation kinetics, and gas filtration through pores:

$$\frac{\partial Y_H}{\partial t} = -\frac{6k_R}{B\rho_H d_0} \frac{P^{eq} - P^0}{1 + \gamma} Y_H^{2/3} \quad (1)$$

where  $Y_H$  is the hydrate conversion degree (the percentage of the remaining gas hydrate),  $k_R$  ( $k_R = k_0 \exp(-E_a/RT)$ ) is the kinetic coefficient of the dissociation rate of the gas hydrate,  $B$  is the initial methane content in the gas hydrate,  $\rho_H$  is the hydrate particle density,  $d_0$  is the average diameter of the gas hydrate particles,  $P^{eq}$  is the equilibrium methane pressure onto the gas hydrate,  $P^0$  is the partial methane pressure, and  $\gamma$  is the coefficient reflecting the impact of pore resistance [55].

We used Equation (1) for modeling the CO<sub>2</sub> hydrate dissociation. The kinetic constants  $k_0$  and  $E_a$  for CO<sub>2</sub> hydrate were taken from Ref. [56]. The theoretical research into the combustion patterns involved typical liquid fuels. The flammable liquid evaporated from a 0.1 × 0.1 m section of the surface. The flame combustion was suppressed by placing a tablet (tablets) or pouring CO<sub>2</sub> hydrate powder on the free surface of the flammable liquid. The granule diameter was 3 mm. The tablet porosity was  $P = 0.3$ , and the granule porosity

was varied in the calculations. A tablet consisted of particles 0.3 mm in diameter. The entire surface of a tablet and the entire surface of a particle (spherical granule) participated in the dissociation. The number of spherical particles (granules) was chosen so that their total mass was equal to the mass of one tablet. The calculations also estimated the number of tablets required for the effective suppression of flame combustion. The following factors affect the fire suppression using CO<sub>2</sub> hydrate: (1) high release rate of carbon dioxide during the gas hydrate dissociation, (2) high water vapor concentration, and (3) heat of phase transitions (water evaporation, ice melting, and gas hydrate dissociation), which leads to flame cooling. Carbon dioxide is released fast at high dissociation rates. We only accounted for the first factor (CO<sub>2</sub> release rate) in the calculations for simplicity. It was assumed that if the first factor led to flame quenching, the remaining two factors (water vapor and phase transitions) would increase the suppression efficiency. The evaluation criteria for the remaining two factors are the subject of further research. To evaluate the suppression based on gas release, we used the ratio  $Z = \frac{V_{CO_2}}{V_{O_2}} > 1$ , where  $V_{CO_2}$  is the carbon dioxide release rate from the entire surface of gas hydrate, and  $V_{O_2}$  is the oxygen flow rate due to air buoyancy.  $V_{O_2}$  can be approximately estimated using Equation (2):

$$V_{O_2} = 0.23\sqrt{2g\beta\Delta T L} \quad (2)$$

where  $L = 0.05$  m, and  $\Delta T$  is the difference between the flame temperature and ambient air temperature. The coefficient 0.23 accounts for the mass concentration of oxygen in the air (about 23%). We assumed that when  $Z > 1$ , there is a significant oxidizer deficiency in the combustion zone, leading to flame extinction.

Figure 18 presents the mathematical curves of the current mass of a CO<sub>2</sub> hydrate tablet and carbon dioxide release rate versus the ambient air temperature  $T$ . The average temperature in the gas vicinity of the tablet is lower than the flame temperature at a distance. Due to the water vapor flow and phase transitions, the temperature around the gas hydrate will decrease. That is why the temperature  $T$  varies from 100 °C to 500 °C. Higher temperature leads to an increase in the heat flux and a decrease in the total dissociation time from 400 s to 50 s. According to the calculations, an increase in temperature up to 700–800 °C will lead to a reduction in the total dissociation time down to 25–35 s, which corresponds to the experiments on tablet dissociation in Figures 2 and 3 (around 20–40 s). The maximum dissociation rate at  $T = 500$  °C corresponds to a time of about 20 s. The mathematical curves on the CO<sub>2</sub> hydrate powder dissociation with varying powder porosity  $P$  and ambient air temperature  $T$  are shown in Figure 19. The experiments in Figures 2 and 3 show that the extinction time is approximately the same (about 20 s) when a tablet and powder are used. This stems from different conditions of the experiment and powder modeling. In the experiments, the powder was poured from a height of about 10 mm and formed an aggregated layer immediately. The maximum temperature was only observed in the vicinity of the powder layer surface. In the calculations, however, powder particles did not affect each other nor interact with each other, and dissociation occurred when the powder fell from a rather great height on a relatively large combustion surface, which is possible during full-scale experiments. Our experiments with a flame height of about 200–300 mm showed that the flame extinction happened within 1–2 s when the powder with a mass of 15 g was poured evenly from a height of 500 mm (the fuel surface area was 150 mm × 100 mm). This time corresponds to Figure 19b at 300–400 °C.

According to the calculation, using Equation (2), the value of  $V_{O_2}$  is about 0.52 m/s. The parameter  $Z > 1$  if 45 tablets are used. Then,  $V_{CO_2} = 0.012 \cdot 45 = 0.54$  m/s (Figure 18b). The mass of one tablet is approximately 1.1 g, and the total mass of tablets will be around 50 g. The maximum carbon dioxide release rate is approximately 0.03 m/s during the dissociation of one gas hydrate granule 3 mm in diameter (Figure 19b). The mass of one tablet (given the tablet and powder porosity) corresponds to the mass of about 61 granules. Then, the total gas release rate for 61 granules will be  $V_{CO_2} = 0.03 \cdot 61 = 1.83$  m/s (Figure 18b). The parameter  $Z = 1.83/0.54 = 3.4$ . In this case, the rapid release of carbon dioxide (a split

second) will be enough for the fast fire suppression due to the absence of the oxidizer flow to the combustion zone. At the same time, it is necessary to provide the even supply of the powder (granules) to the surface of the burning fuel from a height that exceeds the flame height (to ensure the fast dissociation of gas hydrate). The research findings indicate that the suppression of a flame combustion zone using powder with a granule size of about 3 mm will require 20-times less carbon dioxide hydrate than in the case of pressed tablets. The suppression time using the powder is about 1 s. These patterns should be taken into account when planning the use of gas hydrates as extinguishing agents against fires involving flammable liquids and fuel.

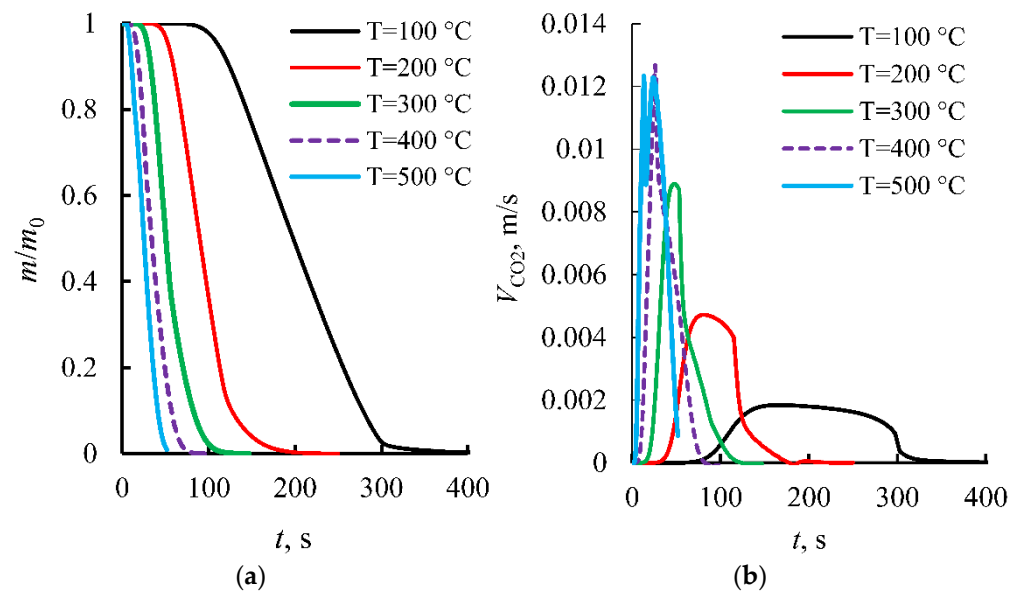


**Figure 18.** (a) Dissociation of a CO<sub>2</sub> hydrate tablet with varying ambient temperature  $T$  ( $m_0$  is the initial mass of gas hydrate, the tablet diameter is 20 mm, and the tablet height is 5–6 mm). (b) Carbon dioxide release rate during the dissociation with varying tablet porosity  $P$  and ambient gas temperature  $T$ .

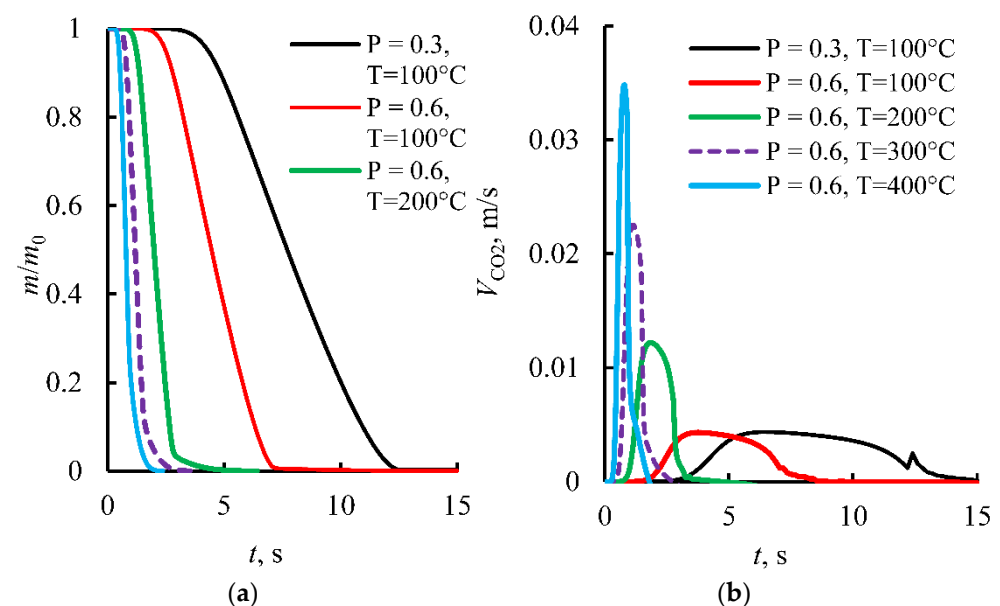


**Figure 19.** (a) Dissociation of CO<sub>2</sub> hydrate powder with varying tablet porosity  $P$  and ambient gas temperature  $T$  ( $m_0$  is the initial mass of gas hydrate; the spherical granule diameter is 3 mm). (b) Carbon dioxide release rate during the dissociation with varying  $P$  and  $T$ .

## 5. Conclusions

- (i) The aim of this research was achieved through several series of experiments with different flammable liquids. When heated, gas hydrates exhibit accelerated dissociation into ice and gas. Dissociation is also accompanied by ice melting, water evaporation, and gas release. This complex set of phase transitions makes it possible to activate any of the liquid combustion suppression mechanisms: reduction in the flammable liquid temperature due to melting and evaporation, access of powder granules to the lower layers of fire, and blocking the oxidizer access by a large amount of carbon dioxide released in the process. A series of experiments demonstrated how the dominating mechanism of liquid pool fire suppression changes with varying mass and type of hydrate (powder, tablets, and spheres).
- (ii) The experiments determined the optimal CO<sub>2</sub> hydrate mass-to-surface area ratio for the containment and suppression of fires involving the most widespread and fire-hazardous flammable liquids: gasoline, kerosene, diesel fuel, oil, and alcohol. CO<sub>2</sub> hydrate powder is found to be more effective than ice, snow, and water/foaming agent emulsion as a fire suppressant in terms of flammable liquid extinction time. The use of CO<sub>2</sub> hydrate in the form of powder for extinguishing flammable liquid pool fires provides a 90–96% shorter extinction time.
- (iii) Fire suppression by CO<sub>2</sub> hydrate powder reduces the CO<sub>2</sub> and CO concentrations by 40% for different flammable liquids due to the additional water vapor from the dissociating gas hydrate joining the reaction.
- (iv) The extinction of a laboratory-scale flammable-liquid pool fire with a fuel film thickness of up to 2 mm requires a CO<sub>2</sub> hydrate discharge density of at least 1.3 kg/m<sup>2</sup>. The specific discharge density required for extinguishing a laboratory-scale pool fire must exceed 0.2 kg/(m<sup>2</sup>·s).
- (v) The CO<sub>2</sub> hydrate dissociation modeling shows that the suppression of a flame using powder with a granule size of about 3 mm will require 20 times less carbon dioxide hydrate than in the case of pressed tablets. The suppression time using powder granules is 1 s.
- (vi) The experimental findings can be used as a database for the development of flammable liquid fire suppression in industrial buildings and warehouses within a short period of time using carbon dioxide hydrate spheres, tablets, and granules.

**Supplementary Materials:** The following supporting information can be downloaded at: <https://www.mdpi.com/article/10.3390/en15249585/s1>.

**Author Contributions:** Conceptualization, data curation, and funding acquisition, S.M.; investigation, S.M., R.V., I.D., V.M., and O.G.; writing—original draft, S.M. and O.G.; writing—review and editing, R.V., S.M., and O.G. All authors have read and agreed to the published version of the manuscript.

**Funding:** This research was supported by the program of the National Research Tomsk Polytechnic University (Priority-2030-NIP/EB-006-0000-2022). Calculations were carried out using the resources of the High-Temperature Circuit Multi-Access Research Center (project No. 13.CKP.21.0038) (Igor Donskoy).

**Conflicts of Interest:** The authors declare no conflict of interest.

## References

1. Ding, F.; Kang, W.; Yan, L.; Xu, Z.; Guo, X. Influence of gas–liquid ratio on the fire-extinguishing efficiency of compressed gas protein foam in diesel pool fire. *J. Therm. Anal. Calorim.* **2021**, *146*, 1465–1472. [[CrossRef](#)]
2. Lu, Y.; Fan, X.; Zhao, Z.; Jiang, X. Dynamic Fire Risk Classification Prediction of Stadiums: Multi-Dimensional Machine Learning Analysis Based On Intelligent Perception. *Appl. Sci.* **2022**, *12*, 6607. [[CrossRef](#)]
3. Chen, M.; Liu, J.; Dongxu, O.; Cao, S.; Wang, Z.; Wang, J. A simplified analysis to predict the fire hazard of primary lithium battery. *Appl. Sci.* **2018**, *8*, 2329. [[CrossRef](#)]

4. Argyropoulos, C.D.; Christolis, M.N.; Nivolianitou, Z.; Markatos, N.C. A hazards assessment methodology for large liquid hydrocarbon fuel tanks. *J. Loss Prev. Process Ind.* **2012**, *25*, 329–335. [[CrossRef](#)]
5. Kwon, K.; Kim, Y.; Kwon, Y.; Koseki, H. Study on accidental fire at a large-scale floating-roof gasoline storage tank. *J. Loss Prev. Process Ind.* **2021**, *73*, 104613. [[CrossRef](#)]
6. Zhou, R.; Dou, X.; Lang, X.; He, L.; Liu, J.; Mu, S. Foaming ability and stability of silica nanoparticle-based triple-phase foam for oil fire extinguishing: Experimental. *Soft Mater.* **2018**, *16*, 327–338. [[CrossRef](#)]
7. Hu, Y.; Zhou, X.; Wu, Z.; Ju, X.; Peng, Y.; Yang, L. Ignition and burning behaviors of automobile oil in engine compartment. *J. Therm. Anal. Calorim.* **2018**, *132*, 305–316. [[CrossRef](#)]
8. Tianwei, Z.; Cunwei, Z.; Hao, L.; Zhiyue, H. Experimental investigation of novel dry liquids with aqueous potassium Solution@Nano-SiO<sub>2</sub> for the suppression of liquid fuel fires: Preparation, application, and stability. *Fire Saf. J.* **2020**, *115*, 103144. [[CrossRef](#)]
9. Von Blottnitz, H.; Curran, M.A. A review of assessments conducted on bio-ethanol as a transportation fuel from a net energy, greenhouse gas, and environmental life cycle perspective. *J. Clean. Prod.* **2007**, *15*, 607–619. [[CrossRef](#)]
10. Kim, D.; Sakimoto, K.K.; Hong, D.; Yang, P. Artificial Photosynthesis for Sustainable Fuel and Chemical Production. *Angew. Chem. Int. Ed.* **2015**, *54*, 3259–3266. [[CrossRef](#)]
11. Shinoda, K.; Nomura, T. Miscibility of fluorocarbon and hydrocarbon surfactants in micelles and liquid mixtures. Basic studies of oil repellent and fire extinguishing agents. *J. Phys. Chem.* **1980**, *84*, 365–369. [[CrossRef](#)]
12. Khoat, H.T.; Kim, J.T.; Quoc, T.D.; Kwark, J.H.; Ryou, H.S. A numerical analysis of the fire characteristics after sprinkler activation in the compartment fire. *Energies* **2020**, *13*, 3099. [[CrossRef](#)]
13. Kim, Y.H.; Lee, M.; Hwang, I.J.; Kim, Y.J. Noise reduction of an extinguishing nozzle using the response surface method. *Energies* **2019**, *12*, 4346. [[CrossRef](#)]
14. Xu, Z.; Guo, X.; Yan, L.; Kang, W. Fire-extinguishing performance and mechanism of aqueous film-forming foam in diesel pool fire. *Case Stud. Therm. Eng.* **2020**, *17*, 100578. [[CrossRef](#)]
15. Wang, H.; Du, Z.; Zhang, T.; Wang, Q.; Li, Y.; Kang, Q. Performance of Foam Agents on Pool Fires at High Altitudes. *Fire Technol.* **2022**, *58*, 1285–1304. [[CrossRef](#)]
16. Rie, D.H.; Lee, J.W.; Kim, S. Class B fire-extinguishing performance evaluation of a compressed air foam system at different air-to-aqueous foam solution mixing ratios. *Appl. Sci.* **2016**, *6*, 191. [[CrossRef](#)]
17. Lv, D.; Tan, W.; Zhu, G.; Liu, L. Gasoline fire extinguishing by 0.7 MPa water mist with multicomponent additives driven by CO<sub>2</sub>. *Process Saf. Environ. Prot.* **2019**, *129*, 168–175. [[CrossRef](#)]
18. Harding, B.; Zhang, B.; Liu, Y.; Chen, H.; Mannan, M.S. Improved research-scale foam generator design and performance characterization. *J. Loss Prev. Process Ind.* **2016**, *39*, 173–180. [[CrossRef](#)]
19. Koshiba, Y.; Okazaki, S.; Ohtani, H. Experimental investigation of the fire extinguishing capability of ferrocene-containing water mist. *Fire Saf. J.* **2016**, *83*, 90–98. [[CrossRef](#)]
20. Rumminger, M.D.; Linteris, G.T. Inhibition of premixed carbon monoxide–hydrogen–oxygen–nitrogen flames by iron pentacarbonyl. *Combust. Flame* **2000**, *120*, 451–464. [[CrossRef](#)]
21. Liu, C. Fire fighting of wind extinguisher with CO<sub>2</sub> gas assisted. *Appl. Mech. Mater.* **2012**, *130–134*, 1054–1057. [[CrossRef](#)]
22. Sloan, E.D., Jr.; Koh, C.A. *Clathrate Hydrates of Natural Gases*, 3rd ed.; CRC Press: Boca Raton, FL, USA; Taylor and Francis Group: Boca Raton, FL, USA, 2008. [[CrossRef](#)]
23. Guo, Z.; Yuan, Y.; Jiang, M.; Liu, J.; Wang, X.; Wang, B. Sensitivity and Resolution of Controlled-Source Electromagnetic Method for Gas Hydrate Stable Zone. *Energies* **2021**, *14*, 8318. [[CrossRef](#)]
24. Li, X.; Wang, C.; Li, Q.; Fan, Q.; Chen, G.; Sun, C. Study on the growth kinetics and morphology of methane hydrate film in a porous glass microfluidic device. *Energies* **2021**, *14*, 6814. [[CrossRef](#)]
25. Li, L.; Li, X.; Wang, Y.; Qin, C.; Li, B.; Luo, Y.; Feng, J. Investigating the interaction effects between reservoir deformation and hydrate dissociation in hydrate-bearing sediment by depressurization method. *Energies* **2021**, *14*, 548. [[CrossRef](#)]
26. Sahith, S.J.K.; Pedapati, S.R.; Lal, B. Investigation on gas hydrates formation and dissociation in multiphase gas dominant transmission pipelines. *Appl. Sci.* **2020**, *10*, 5052. [[CrossRef](#)]
27. Lv, X.; Shi, B.; Zhou, S.; Wang, S.; Huang, W.; Sun, X. Study on the decomposition mechanism of natural gas hydrate particles and its microscopic agglomeration characteristics. *Appl. Sci.* **2018**, *8*, 2464. [[CrossRef](#)]
28. Rossi, F.; Gambelli, A.M.; Sharma, D.K.; Castellani, B.; Nicolini, A.; Castaldi, M.J. Experiments on methane hydrates formation in seabed deposits and gas recovery adopting carbon dioxide replacement strategies. *Appl. Therm. Eng.* **2019**, *148*, 371–381. [[CrossRef](#)]
29. Kang, K.C.; Linga, P.; Park, K.-N.; Choi, S.J.; Lee, J.D. Seawater desalination by gas hydrate process and removal characteristics of dissolved ions (Na<sup>+</sup>, K<sup>+</sup>, Mg<sup>2+</sup>, Ca<sup>2+</sup>, B<sup>3+</sup>, Cl<sup>-</sup>, SO<sub>4</sub><sup>2-</sup>). *Desalination* **2014**, *353*, 84–90. [[CrossRef](#)]
30. Liu, N.; Meng, F.; Chen, L.; Yang, L.; Liu, D. Investigating the effects of MWCNT-HB on gas storage performance of CO<sub>2</sub> hydrate. *Fuel* **2022**, *316*, 123289. [[CrossRef](#)]
31. Zhang, X.; Wang, J.; Yang, H.; Li, J.; Li, Y.; Wu, Q. Formation and storage characteristics of CO<sub>2</sub> hydrate in porous media: Effect of liquefaction amount on the formation rate, accumulation amount. *Appl. Therm. Eng.* **2022**, *214*, 118747. [[CrossRef](#)]
32. Prah, B.; Yun, R. CO<sub>2</sub> hydrate slurry transportation in carbon capture and storage. *Appl. Therm. Eng.* **2018**, *128*, 653–661. [[CrossRef](#)]
33. Sato, T.; Takeya, S.; Nagashima, H.D.; Ohmura, R. Preservation of carbon dioxide clathrate hydrate coexisting with sucrose under domestic freezer conditions. *J. Food Eng.* **2014**, *120*, 69–74. [[CrossRef](#)]

34. Choi, J.W.; Kim, S.; Kang, Y.T. CO<sub>2</sub> hydrate cooling system and LCC analysis for energy transportation application. *Appl. Therm. Eng.* **2015**, *91*, 11–18. [[CrossRef](#)]
35. Liu, R.; Gao, F.; Liang, K.; Yuan, Z.; Ruan, C.; Wang, L.; Yang, S. Experimental study on the correlation between rapid formation of gas hydrate and diffusion of guest molecules. *Appl. Therm. Eng.* **2019**, *154*, 393–399. [[CrossRef](#)]
36. Wei, J.; Cheng, Y.; Yan, C.; Li, Q.; Han, S.; Ansari, U. Decomposition prevention through thermal sensitivity of hydrate formations around wellbore. *Appl. Therm. Eng.* **2019**, *159*, 113921. [[CrossRef](#)]
37. Hatakeyama, T.; Aida, E.; Yokomori, T.; Ohmura, R.; Ueda, T. Fire extinction using carbon dioxide hydrate. *Ind. Eng. Chem. Res.* **2009**, *48*, 4083–4087. [[CrossRef](#)]
38. Sugahara, A.; Nakano, H.; Yokomori, T.; Ohmura, R.; Ueda, T. Effect of fuel boiling point of pool flame for the flame extinction by CO<sub>2</sub> hydrate. In Proceedings of the ASPACC 2015—10th Asia-Pacific Conference on Combustion, Beijing, China, 19–22 July 2015.
39. GOST 32513-2013; Automotive Fuels. Unleaded Petrol. Specifications. Federal Agency for Technical Regulation and Metrology: Moscow, Russia, 2015.
40. GOST 10227-86; Jetfuels. Specifications. Federal Agency for Technical Regulation and Metrology: Moscow, Russia, 1987.
41. GOST 305-82; Diesel Fuel. Specifications. Federal Agency for Technical Regulation and Metrology: Moscow, Russia, 1982.
42. GOST 5962-2013; Rectified Ethyl Alcohol from Edible Raw Material. Specifications. Federal Agency for Technical Regulation and Metrology: Moscow, Russia, 2013.
43. Jayasuriya, J.; Moser, I.; de Mel, R. An automated water dispensing system for controlling fires in coal yards. *Int. J. Coal Sci. Technol.* **2022**, *9*, 23. [[CrossRef](#)]
44. Liu, Y.; Fu, Z.; Zheng, G.; Chen, P. Study on the effect of mist flux on water mist fire extinguishing. *Fire Saf. J.* **2022**, *130*, 103601. [[CrossRef](#)]
45. Qin, Y.; Guo, W.; Xu, H.; Song, Y.; Chen, Y.; Ma, L. A comprehensive method to prevent top-coal spontaneous combustion utilizing dry ice as a fire extinguishing medium: Test apparatus development and field application. *Environ. Sci. Pollut. Res.* **2022**, *29*, 19741–19751. [[CrossRef](#)]
46. Tupsakhare, S.S.; Castaldi, M.J. Efficiency enhancements in methane recovery from natural gas hydrates using injection of CO<sub>2</sub>/N<sub>2</sub> gas mixture simulating in-situ combustion. *Appl. Energy* **2019**, *236*, 825–836. [[CrossRef](#)]
47. Misyura, S.Y.; Manakov, A.Y.; Morozov, V.S.; Nyashina, G.S.; Gaidukova, O.S.; Skiba, S.S.; Volkov, R.S.; Voytkov, I.S. The influence of key parameters on combustion of double gas hydrate. *J. Nat. Gas Sci. Eng.* **2020**, *80*, 103396. [[CrossRef](#)]
48. Misyura, S.Y.; Donskoy, I.G. Improving the efficiency of storage of natural and artificial methane hydrates. *J. Nat. Gas Sci. Eng.* **2022**, *97*, 104324. [[CrossRef](#)]
49. Kuhs, W.F.; Genov, G.; Staykova, D.K.; Hansen, T. Ice perfection and onset of anomalous preservation of gas hydrates. *Phys. Chem. Chem. Phys.* **2004**, *6*, 4917–4920. [[CrossRef](#)]
50. Takeya, S.; Yoneyama, A.; Ueda, K.; Mimachi, H.; Takahashi, M.; Sano, K.; Hyodo, K.; Takeda, T.; Gotoh, Y. Anomalously preserved clathrate hydrate of natural gas in pellet form at 253 K. *J. Phys. Chem. C* **2012**, *116*, 13842–13848. [[CrossRef](#)]
51. Misyura, S.Y.; Donskoy, I.G.; Manakov, A.Y.; Morozov, V.S.; Strizhak, P.A.; Skiba, S.S.; Sagidullin, A.K. Studying the influence of key parameters on the methane hydrate dissociation in order to improve the storage efficiency. *J. Energy Storage* **2021**, *44*, 103288. [[CrossRef](#)]
52. Cui, G.; Dong, Z.; Wang, S.; Xing, X.; Shan, T.; Li, Z. Effect of the water on the flame characteristics of methane hydrate combustion. *Appl. Energy* **2020**, *259*, 114205. [[CrossRef](#)]
53. Wu, F.H.; Padilla, R.E.; Dunn-Rankin, D.; Chen, G.B.; Chao, Y.C. Thermal structure of methane hydrate fueled flames. *Proc. Combust. Inst.* **2017**, *36*, 4391–4398. [[CrossRef](#)]
54. Misyura, S.Y.; Donskoy, I.G. Co-modeling of methane hydrate dissociation and combustion in a boundary layer. *Combust. Flame* **2022**, *238*, 111912. [[CrossRef](#)]
55. Misyura, S.Y.; Donskoy, I.G. Dissociation of a powder layer of methane gas hydrate in a wide range of temperatures and heat fluxes. *Powder Technol.* **2022**, *397*, 117017. [[CrossRef](#)]
56. Misyura, S.Y.; Donskoy, I.G. Dissociation kinetics of methane hydrate and CO<sub>2</sub> hydrate for different granular composition. *Fuel* **2020**, *262*, 116614. [[CrossRef](#)]